AIP Advances

Local droplet etching on InAlAs/InP surfaces with InAl droplets

Cite as: AIP Advances **12**, 055302 (2022); https://doi.org/10.1063/5.0088012
Submitted: 16 March 2022 • Accepted: 11 April 2022 • Published Online: 02 May 2022

Xin Cao, Yiteng Zhang, Chenxi Ma, et al.

COLLECTIONS

EP This paper was selected as an Editor's Pick

ARTICLES YOU MAY BE INTERESTED IN

Single photon emission from ODT passivated near-surface GaAs quantum dots
Applied Physics Letters **118**, 221107 (2021); https://doi.org/10.1063/5.0046042

GaAs quantum dots grown by droplet etching epitaxy as quantum light sources
Applied Physics Letters **119**, 120502 (2021); https://doi.org/10.1063/5.0057070

Progress in quantum-dot single photon sources for quantum information technologies: A broad spectrum overview
Applied Physics Reviews **7**, 021309 (2020); https://doi.org/10.1063/5.0010193

© 2022 Author(s).

Local droplet etching on InAlAs/InP surfaces with InAl droplets

Cite as: AIP Advances 12, 055302 (2022); doi: 10.1063/5.0088012
Submitted: 16 March 2022 • Accepted: 11 April 2022 •
Published Online: 2 May 2022

View Online

Export Citation

CrossMark

Xin Cao,[1] Yiteng Zhang,[1] Chenxi Ma,[1] Yinan Wang,[1] Benedikt Brechtken,[1] Rolf J. Haug,[1,2] Eddy P. Rugeramigabo,[1] Michael Zopf,[1,a)] and Fei Ding[1,2,a)]

AFFILIATIONS

[1] Institut für Festkörperphysik, Leibniz Universität Hannover, Appelstraße 2, 30167 Hannover, Germany
[2] Laboratorium für Nano- und Quantenengineering, Leibniz Universität Hannover, Schneiderberg 39, 30167 Hannover, Germany

[a)] **Authors to whom correspondence should be addressed:** michael.zopf@fkp.uni-hannover.de and fei.ding@fkp.uni-hannover.de

ABSTRACT

GaAs quantum dots (QDs) grown by local droplet etching (LDE) have been studied extensively in recent years. The LDE method allows for high crystallinity, as well as precise control of the density, morphology, and size of QDs. These properties make GaAs QDs an ideal candidate as single photon and entangled photon sources at short wavelengths (<800 nm). For technologically important telecom wavelengths, however, it is still unclear whether LDE grown QDs can be realized. Controlling the growth conditions does not enable shifting the wavelength of GaAs QDs to the telecom region. New recipes will have to be established. In this work, we study Indium–Aluminum (InAl) droplet etching on ultra-smooth $In_{0.55}Al_{0.45}As$ surfaces on InP substrates, with a goal to lay the foundation for growing symmetrical and strain-free telecom QDs using the LDE method. We report that both droplets start to etch nanoholes at a substrate temperature above 415 °C, showing varying nanohole morphology and rapidly changing density (by more than one order of magnitude) at different temperatures. Al and In droplets are found to not intermix during etching, and instead etch nanoholes individually. The obtained nanoholes show a symmetric profile and very low densities, enabling infilling of lattice-matched InGaAs QDs on $In_xAl_{1-x}As$/InP surfaces in further works.

© 2022 Author(s). All article content, except where otherwise noted, is licensed under a Creative Commons Attribution (CC BY) license (http://creativecommons.org/licenses/by/4.0/). https://doi.org/10.1063/5.0088012

Epitaxial III–V semiconductor quantum dots (QDs) have been actively studied for decades.[1,2] They are considered as an ideal candidate for quantum information processing applications.[3–5] Their electronic and optical properties are highly related to the growth procedure, making a careful and deterministic development thereof indispensable. Epitaxially grown QDs can be obtained in a variety of ways, such as by quantum well thickness fluctuations ("natural" QDs),[6] self-assembly using the Stranski–Krastanov (S–K) method[7] or droplet epitaxy (DE),[8] nanopatterning,[9] and QD infilling in nanoholes created by local droplet etching (LDE).[10] Natural QDs mostly appear in the GaAs/AlGaAs and GaAs/AlAs quantum wells,[6,11] where the monolayer thickness fluctuations lead to the formation of local confinement potentials. The S–K method relies on a lattice mismatch between the QD and the substrate. The residual strain fields in the QD as well as their morphology tend to be inhomogeneous and asymmetric, resulting in an inhomogeneous emission broadening and the notorious exciton fine structure splitting (FSS).[12] The latter sets a limitation to the achievable *steady-state* entanglement fidelity of polarization-entangled photon pairs emitted by the QDs.[13] With careful optimization of the growth parameters, S–K grown QDs with low FSS have been reported, for example, in the InAs/InP system.[14] Droplet epitaxy was first used to grow GaAs microcrystals[15] and strain-free GaAs/AlGaAs QDs.[16] Both strained and unstrained QDs can be grown via the DE method with low FSSs at various wavelengths.[12,17] Nanopatterning by lithography has the advantage of site-controlled growth of QDs.[9,18,19] However, a number of detrimental effects, such as the interfacial damages and defects, are unavoidable during the *ex-situ* etching, degrading the optical properties of QDs.[20]

Another promising method is to infill QDs in the LDE induced nanoholes. Here, the nanoholes are etched *in situ* during the sample growth, thus maintaining a high crystallinity. The LDE method was first observed during the droplet epitaxy at high temperatures.[21] At sufficiently high substrate temperature and without the supply

of group V elements, metal droplets act as "electrochemical drills" and etch nanoholes on the surface due to desorption of group V elements underneath the droplets. Under such ultrahigh vacuum epitaxial conditions, interfacial defects are avoided, leading to a *defect-free* "nanopatterning." The lateral dimension of the etched nanoholes is much larger than the vertical dimension. After infilling the nanoholes with the target materials, QDs are formed with the charge carriers weakly confined in the lateral direction. The QD emission energy can be precisely controlled, simply by adjusting with the infilling amount.[10] By infilling the nanoholes with lattice matched material, strain-free QDs can be obtained. These properties lead to a highly deterministic set of optical properties, with ultra-low statistical deviation in the emission wavelength and FSS.[22]

Local droplet etching has been systematically studied in the GaAs/AlGaAs system in the last decade.[23–27] Various droplets, such as Al,[28] In,[29] Ga,[24] and InGa alloys,[30] have been reported to etch nanoholes on GaAs and AlGaAs surfaces. Nanoholes etched by the Al droplets are more symmetric in morphology than the ones etched by Ga, resulting in GaAs QDs with ultra-small FSSs[31] and high entanglement fidelities without the need for post-growth tuning.[22] QDs formed in the defect and impurity-free nanoholes yield the purest single photon emission with $g^{(2)}(0) \sim 10^{-5}$ [4] and a high single photon indistinguishability of 0.95 (raw value).[32] However, these GaAs QDs emit photons in the 700–800 nm range, while the envisioned long-haul quantum communication (and, possibly, the coupling with mature silicon photonics) requires photons at the telecom O-band or C-band. In this regard, GaSb/AlGaSb and In(Ga)As/InAlAs/InP-based materials are particularly interesting owing to their small direct band gaps and wide possibilities of band engineering. QDs emitting at the telecom wavelengths have been demonstrated with these materials, by using the S–K, DE, and nanopatterning methods.[18,33–37] However, it is still unclear whether the LDE grown QDs can be realized with either GaSb/AlGaSb or In(Ga)As/InAlAs/InP.[38] New recipes will have to be established. There are two main challenges: (1) the growth of *lattice-matched* and *defect-free* layers on the substrate and (2) the LDE etching of nanoholes.

Here, we study InAl droplet etching of ultra-smooth $In_{0.55}Al_{0.45}As$ layer grown on the InP substrate, which is a key prerequisite for strain-free InGaAs QDs emitting at telecom wavelengths. We notice that, very recently, the LDE etching has been successfully demonstrated on AlGaSb.[39] However, the LDE on InP or InAlAs has not been reported so far. We find that the LDE process on InAlAs has a narrower temperature window than on AlGaSb and AlGaAs systems.[39,40] Al and In droplets etch nanoholes with different morphologies. The depth of the nanoholes increases with etching temperature, and the nanohole density changes by more than one order of magnitude within the temperature window. We, thus, determine the optimum growth conditions for obtaining smooth surfaces and nanoholes with controllable morphology, removing a main obstacle to infilling lattice-matched InGaAs in further works.

The samples are fabricated on semi-insulating InP (001) substrates (Wafer Technology, Ltd.) with solid source molecular beam epitaxy (MBE, Riber Compact 21) system. The substrate surface is deoxidized with the appearance of a neat 4 × RHEED pattern under an As4 flux at 505 °C. The substrate temperature is then decreased to 455 °C, followed by the growth of a 300 nm $In_{0.52}Al_{0.48}As$ lattice-matched buffer layer with a deposition rate of 0.1 nm/s. After that, 200 nm of $In_xAl_{1-x}As$ is deposited as a high bandgap barrier layer. To perform local droplet etching, the arsenic flux is stopped for 15 s to create a low As pressure environment. In and Al molecules, with a nominal total thickness of 0.3 nm, are then supplied together or separately. A small portion of the metal molecules is consumed by the background As molecules while flying toward the substrate. Most of the metal molecules arrive at the substrate and form droplets. Because of the low arsenic background pressure and the high substrate temperature, the covalent bonds of material underneath the droplets break. Driven by the concentration gradient, arsenic from the InAlAs layer migrates to the surface of metal droplets, where it forms covalent bonds again. This induces the nanoholes on the surface. The residual droplets repeat such process and drill deeper holes. After two minutes of etching, arsenic is supplied again to react with the residual metal droplets for another minute. This leads to the crystallization of ring-shaped structures around the nanoholes. Finally, the substrate is cooled down immediately to maintain the morphology of the sample surface. The sketch of the sample structure is shown in Fig. 1(a).

The first and foremost challenge is to realize a smooth and strain-relaxed surface for the subsequent droplet etching. This will be a crucial step to growing strain-free QDs by the LDE method in a lattice matched system. In addition, a smooth surface allows a controllable and reproducible tuning of the QD emission wavelength by modifying the infilling amount in the nanoholes.[10] Last but not least, smooth surfaces with fewer defects are important for achieving high-quality single QD emissions. The defects may bring trap states near the QDs, thus creating non-radiative decay channels and degrading the QD emission. Figures 1(b), 1(d), and 1(f) show the atomic force microscopy (AFM, Veeco, NanoScope V) images of the $In_{0.5}Al_{0.5}As$ $In_{0.55}Al_{0.45}As$ and $In_{0.6}Al_{0.4}As$ surface, respectively. Due to the lattice mismatching, the $In_xAl_{1-x}As$ layer on InP substrate will undergo tensile strain if the In content x is <0.52, and compressive strain if $x > 0.52$.

In the tensile strain region [x = 0.5, see Fig. 1(b)], cracking occurs because the accumulated misfit stress exceeds the elastic limit.[41] High density cracks, with a depth of about 1 nm, are formed along both $[1\bar{1}0]$ and [110] directions, resulting in a root-mean-square (rms) roughness of 0.504 nm. In the compressive strain region, cross hatch patterns typically occur due to the formation of misfit dislocations and penetration of threading dislocations.[42–44] However, in our case, this effect is minimized by introducing the $In_{0.52}Al_{0.48}As$ buffer and carefully tweaking the growth condition for the $In_{0.55}Al_{0.45}As$ layer. The resulting surface is very smooth, with a minimal thickness fluctuation and an excellent rms roughness of 0.146 nm [Figs. 1(d) and 1(e)]. For the strongly compressed $In_{0.6}Al_{0.4}As$ layer, the strain relaxation is significant, leading to large defects along $[1\bar{1}0]$ together with some holes [Fig. 1(f)]. This strong anisotropic strain relaxation was also reported previously.[45]

The second challenge, which will be addressed in the following, is to demonstrate high-quality droplet etching on the obtained $In_{0.55}Al_{0.45}As$ layer. According to the previous studies,[46] $In_{0.55}Ga_{0.45}As$ will emit in the telecom C-band at cryogenic temperatures and is therefore an ideal infilling material for realizing strain-free QDs with the LDE method. To achieve lattice matching, the barrier material must be carefully chosen. We have shown in

© Author(s) 2022

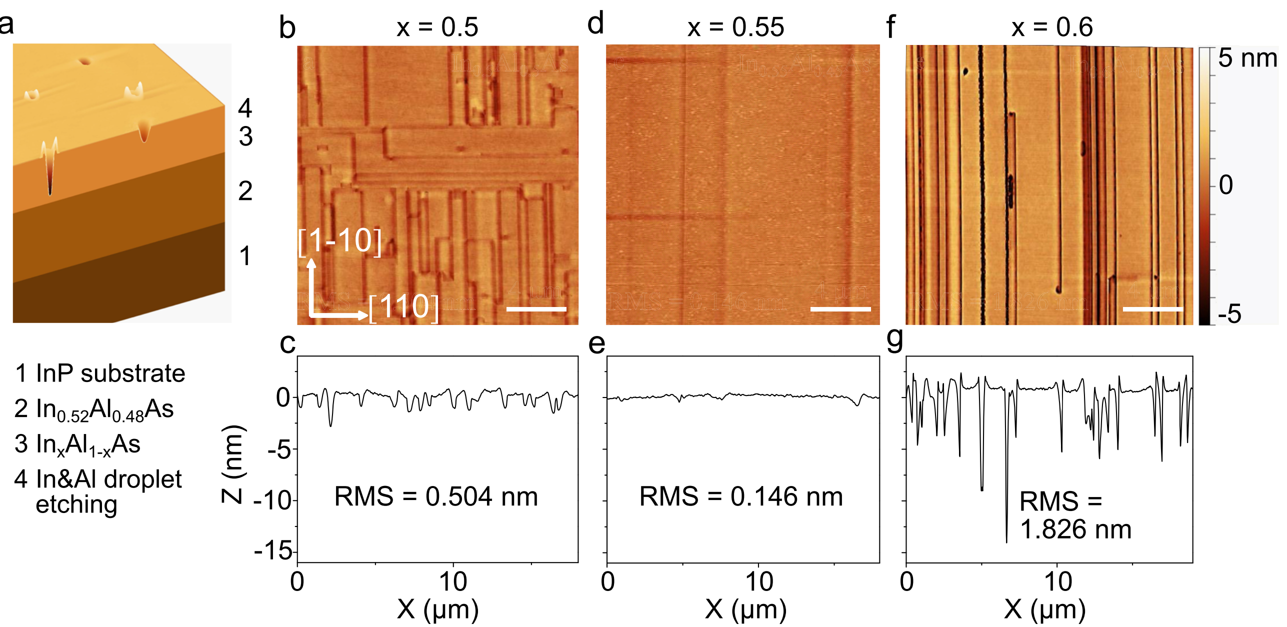

FIG. 1. (a) Sketch of the sample structure. (b), (d), and (f) Atomic force microscopy images of the $In_xAl_{1-x}As$ layer grown on InP substrates. Scale bar: 4 μm. (c), (e), and (g) Line profile of the $In_xAl_{1-x}As$ layers from (b), (d), and (f).

Fig. 1 that $In_{0.55}Al_{0.45}As$, which has nearly the same lattice constant to $In_{0.55}Ga_{0.45}As$, can be grown with very high quality. Therefore, $In_{0.55}Al_{0.45}As$ layers are chosen for the droplet etching studies in the following.

Inspired by the previous work on In_xGa_{1-x} co-droplet etching of GaAs and AlGaAs layers,[30] we choose InAl droplets for the etching of $In_{0.55}Al_{0.45}As$. In our works, $In_{0.55}Al_{0.45}$ droplets are supplied by opening the In and Al cell shutters simultaneously. Substrate temperature is an important parameter for the etching process. Figure 2 displays the AFM images for the etching results obtained at different temperatures. At T = 415 °C, only two types of droplets can be observed at the surface, exhibiting different lateral profiles [Fig. 2(a)]. No nanoholes can be observed. However, when looking at the line profiles of these two droplets, a dip in the middle of the

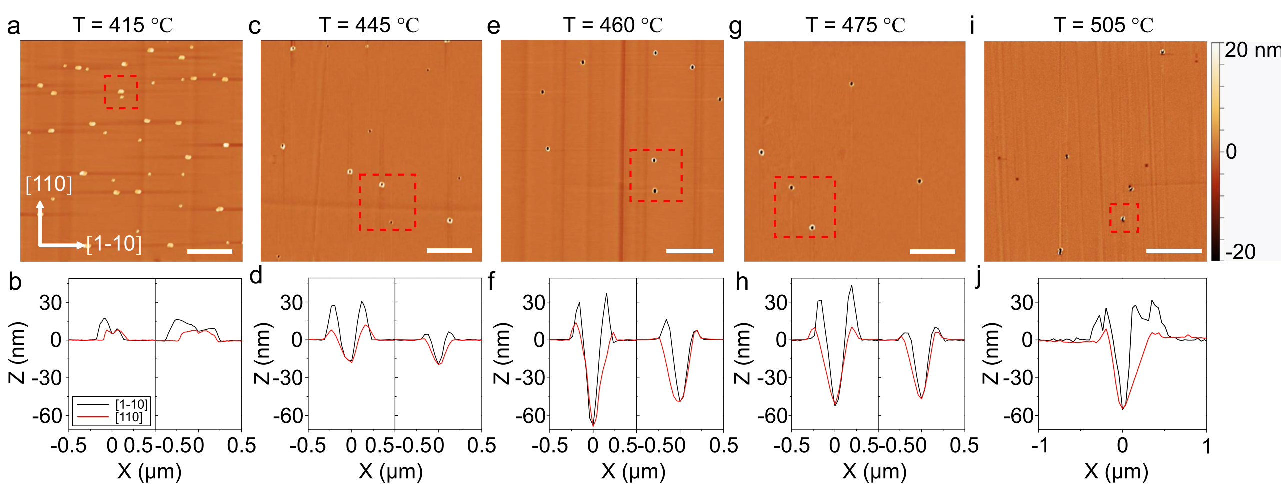

FIG. 2. (Upper row) AFM images of the $In_{0.55}Al_{0.45}As$ surfaces after InAl droplet etching at different temperatures. Scale bar: (a), (c), (e), and (g) 4 μm; (i) 10 μm. (Bottom row) Line profile of two different types of structures (indicated by the red dashed squares in the upper row).

© Author(s) 2022

droplet is observable, indicating the starting of the nanohole etching process [Fig. 2(b)].

According to the previous LDE studies on GaAs QDs at short wavelengths, we suspect that the covalent bond of InAlAs should break at a higher temperature so that the As atoms are free during the etching process. Therefore, the substrate temperature T is increased to 445 °C, with the goal to offer enough thermal energy to break the chemical bonds. Two types of nanoholes are successfully obtained, with ring-shaped structures of different heights formed around them [Figs. 2(c) and 2(d)]. By increasing T to 460 and 475 °C, the morphology of these two types of nanoholes do not change significantly, but the hole depths are increased [Figs. 2(e)–2(h)]. At T = 505 °C, the two types of nanoholes merge seem to together [see also the discussion of Fig. 3(g)] and can be hardly distinguished by their morphology.

At all etching temperatures, the droplets and nanoholes are morphologically asymmetric along the [110] and [1$\bar{1}$0] directions: The ring is higher in the [1$\bar{1}$0] direction while the nanoholes are slightly elongated along the [110] direction. This is because the group III atoms diffuse easier along the [110] direction[47] during the As desorption process. The symmetry of the nanoholes defines the symmetry of the infilled QDs and is therefore related also to the exciton fine structure splitting in the biexciton–exciton cascade process, affecting the polarization entanglement fidelity. The nanohole symmetries shown in Figs. 2(e) and 2(g) are satisfactory but can be further optimized by fine tuning the droplet deposition rate as well as the As pressure during etching.[31,48]

Noting that two types of droplets or nanoholes exist in the etching results, we suspect the In and Al droplets do not intermix during the etching process. This observation is clearly contrary to the previous results on the InGa droplet etching of GaAs and AlGaAs layers.[30] To confirm this, we performed a set of LDE experiments with either In or Al droplets, all at a temperature of 445 °C. The AFM images after the In etching and Al etching are shown in Figs. 3(a) and 3(b), respectively.

Instead of two types of nanoholes as in Fig. 2(c), now only one type exists in each sample. For the In etched nanoholes [Fig. 3(a)], the ring is higher than that of the Al-etched holes [Fig. 3(b)]. The same situation can be observed in Fig. 2, confirming that In and Al droplets etch nanoholes separately even when both materials are supplied simultaneously. This may due to the fact that, for pure metal droplets, the solid solubility of In in Al is 0, restricting the formation of InAl droplets.[49]

In order to gain a deeper understanding of the etching results, scanning electron microscopy (SEM, Raith Pionner Two) was performed for these two types of samples. The backscattered electron (BSE) images and the secondary electron (SE) images are shown in the upper and lower rows of Fig. 3, respectively. The goal is to obtain further information about the material composition of the structures. In the BSE images [Figs. 3(c), 3(e), and 3(g)], there is a strong brightness contrast between the two types of nanoholes, which is a result of the atomic number difference between In and Al. To confirm that such contrast does not stem from the distinct morphology of the droplets or rings, SE images are also collected at the same sample position [Figs. 3(d), 3(f), and 3(h)]. The brightness contrast is now much weaker than that in the BSE images, proving that the contrast in the BSE signal is mainly due to atomic number differences. Interestingly, the nanoholes etched by In droplets and Al droplets at 505 °C [Fig. 3(g)] can be now clearly distinguished [see also Fig. 2(i)]. There is a tendency for these two kinds of droplets to merge at this high temperature—a process that is most probably assisted by a small amount of As supply from the desorption from the underlying

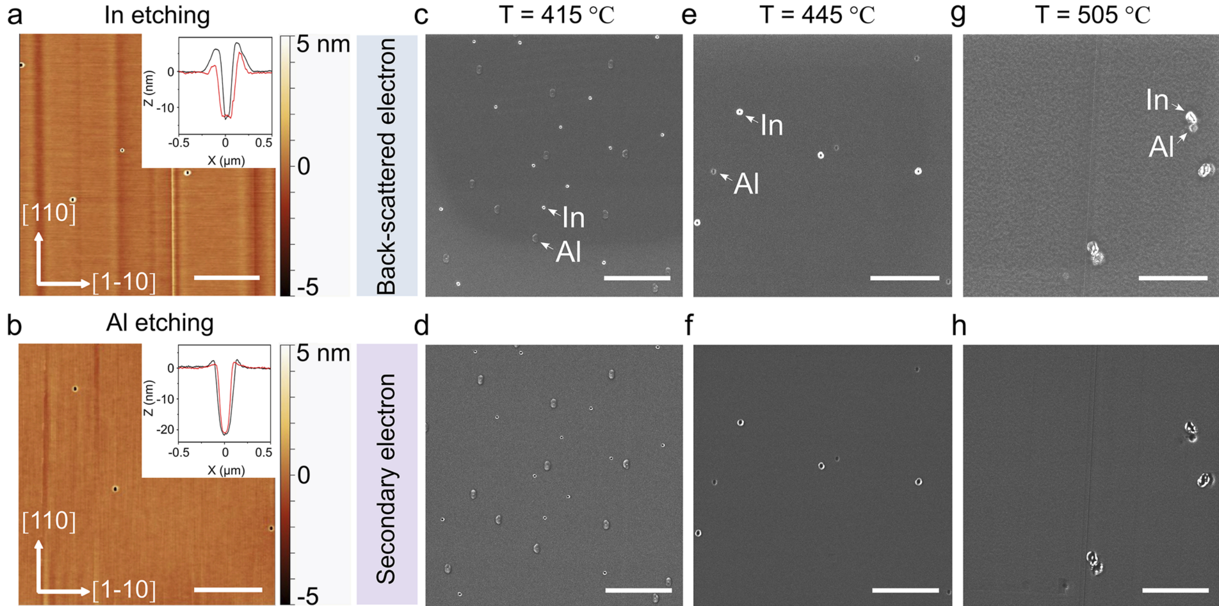

FIG. 3. (a) and (b) AFM images of nanoholes on the InAlAs surfaces that were etched by using (a) 0.167 nm of In and (b) 0.133 nm of Al. Inset: Line profile of the etched nanohole. (c), (e), and (g) SEM images obtained from the back-scattered electron signal, and (d), (f), and (h) from the secondary electrons. Scale bar: 4 μm.

© Author(s) 2022

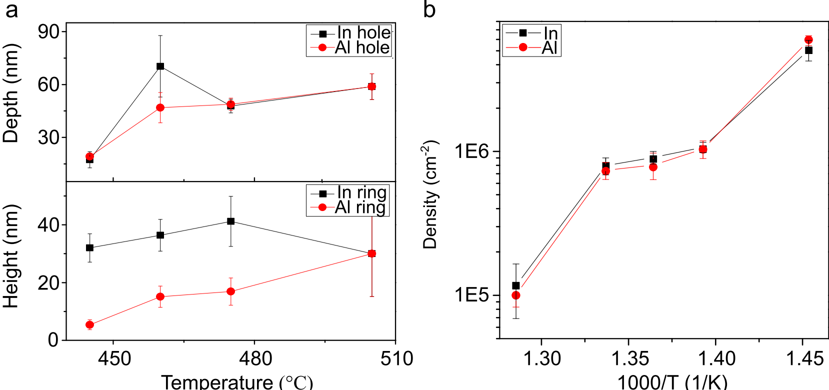

FIG. 4. (a) Depth of the nanoholes and height of the rings, as a function of temperature. The depth is measured from the flat surface to the bottom of the nanohole, and the height is from the flat surface to the top of the ring. (b) Density of holes or droplets as a function of temperature.

layer. The results in Fig. 3 are consistent with that in Fig. 2, proving a strong evidence that the nanoholes with higher (lower) rings in Fig. 2 are due to the In (Al) droplet etching process.

Now, the question is which droplet etching is more suitable for the LDE growth of InGaAs QDs on InAlAs. To answer this, we quantitatively analyze the morphology changes with temperature. The average nanohole depth and ring height are extracted and plotted in Fig. 4(a). Note that the data converge at T = 505 °C due to the inability to distinguish the two types of holes. Both In and Al etched nanoholes show a tendency of becoming deeper with the increasing temperature. This is due to the enhanced thermal energy of arsenic underneath the droplets, which facilitates the migration and desorption of materials from the surface. Here, we also need to consider another known effect for the LDE etching process: at higher temperatures, the big droplets with large depth will form, but at intermediate temperatures, the smaller droplets may drill even deeper due to the smaller contact area. There is a trade-off between a yet small droplet diameter and sufficiently strong arsenic migration, which explains the relatively large depth of In etched nanoholes at 460 °C. This effect is, however, not significant for the Al etched holes. On the other hand, the height of the rings also increases with temperature. At T = 445 °C, the height is 5.4 nm for the Al rings and 32 nm for the In rings. When T is increased to 475 °C, the height is increased to 16.9 and 41.2 nm, respectively. Due to the slight In/Al intermixing at 505 °C, it is difficult to distinguish the two values. Finally, the density changes by nearly two orders of magnitude with temperature, from 6×10^6 cm^{-2} at 415 °C to 1×10^5 cm^{-2} at 505 °C, as shown in Fig. 4(b). This ultra-low density achieved here is a significant advantage for the quantum photonics application of single QDs.

In conclusion, we investigated local droplet etching of ultra-smooth $In_xAl_{1-x}As$ surfaces on InP substrates by using In/Al droplets at etching temperatures between 415 and 505 °C. In contrast to the well-studied In_xGa_{1-x} droplet etching of GaAs and AlGaAs layers, the Al and In droplets in our case do not intermix at temperatures below 500 °C, leading to the formation of two distinct types of nanoholes. Al etched nanoholes have lower ring-like structures around them, which was further confirmed by individual experiments with In and Al droplets. According to the previous studies, the lower rings can facilitate material migration inside the nanoholes during a subsequent infilling process. The obtained nanoholes also show a symmetric profile and very low densities, allowing the infilling of lattice-matched InGaAs. This work represents a crucial step to the demonstration of LDE growth of symmetrical and strain-free QDs at telecom wavelengths.

The authors acknowledge the funding by the German Federal Ministry of Education and Research (BMBF) within the project Q.Link.X (Grant No. 16KIS0869) and QR.X (Grant No. 16KISQ015), the European Research Council (Grant No. QD-NOMS GA715770), and the German Research Foundation under Germany's Excellence Strategy—EXC-2123, Quantum Frontiers—Grant Nos. 390837967 and 454635269. Y. Zhang acknowledges the China Scholarship Council (Grant No. CSC201908370225).

AUTHOR DECLARATIONS

Conflict of Interest

The authors have no conflicts to disclose.

Author Contributions

X.C. and Y.Z. contributed equally to this work.

DATA AVAILABILITY

The data that support the findings of this study are available from the corresponding authors upon reasonable request.

REFERENCES

[1] A. Kumar, S. E. Laux, and F. Stern, Phys. Rev. B **42**, 5166 (1990).
[2] T. Fukui, S. Ando, Y. Tokura, and T. Toriyama, Appl. Phys. Lett. **58**, 2018 (1991).
[3] X. Ding, Y. He, Z. C. Duan, N. Gregersen, M. C. Chen, S. Unsleber, S. Maier, C. Schneider, M. Kamp, S. Höfling, C. Y. Lu, and J. W. Pan, Phys. Rev. Lett. **116**, 020401 (2016).
[4] L. Schweickert, K. D. Jöns, K. D. Zeuner, S. F. Covre Da Silva, H. Huang, T. Lettner, M. Reindl, J. Zichi, R. Trotta, A. Rastelli, and V. Zwiller, Appl. Phys. Lett. **112**, 093106 (2018).
[5] D. Huber, M. Reindl, S. F. Covre Da Silva, C. Schimpf, J. Martín-Sánchez, H. Huang, G. Piredda, J. Edlinger, A. Rastelli, and R. Trotta, Phys. Rev. Lett. **121**, 033902 (2018).

© Author(s) 2022

[6]A. Zrenner, L. V. Butov, M. Hagn, G. Abstreiter, G. Böhm, and G. Weimann, Phys. Rev. Lett. **72**, 3382 (1994).
[7]K. Yamaguchi, K. Yujobo, and T. Kaizu, Jpn. J. Appl. Phys. **39**, L1245 (2000).
[8]N. Koguchi, S. Takahashi, and T. Chikyow, J. Cryst. Growth **111**, 688 (1991).
[9]A. Turala, P. Regreny, P. Rojo-Romeo, C. Priester, and M. Gendry, in *Conference Proceedings–International Conference on Indium Phosphide and Related Materials* (IEEE, 2006), Vol. 214.
[10]P. Atkinson, E. Zallo, and O. G. Schmidt, J. Appl. Phys. **112**, 054303 (2012).
[11]K. Brunner, U. Bockelmann, G. Abstreiter, M. Walther, G. Böhm, G. Tränkle, and G. Weimann, Phys. Rev. Lett. **69**, 3216 (1992).
[12]J. Skiba-Szymanska, R. M. Stevenson, C. Varnava, M. Felle, J. Huwer, T. Müller, A. J. Bennett, J. P. Lee, I. Farrer, A. B. Krysa, P. Spencer, L. E. Goff, D. A. Ritchie, J. Heffernan, and A. J. Shields, Phys. Rev. Appl. **8**, 014013 (2017).
[13]J. Yang, M. Zopf, P. Li, N. L. Sharma, W. Nie, F. Benthin, T. Fandrich, E. P. Rugeramigabo, C. Hopfmann, R. Keil, O. G. Schmidt, and F. Ding, arXiv:2109.06742v1 (2021).
[14]A. Kors, J. P. Reithmaier, and M. Benyoucef, Appl. Phys. Lett. **112**, 172102 (2018).
[15]N. Koguchi and K. Ishige, Jpn. J. Appl. Phys. **32**, 2052 (1993).
[16]F. Basso Basset, S. Bietti, M. Reindl, L. Esposito, A. Fedorov, D. Huber, A. Rastelli, E. Bonera, R. Trotta, and S. Sanguinetti, Nano Lett. **18**, 505 (2018).
[17]M. Gurioli, Z. Wang, A. Rastelli, T. Kuroda, and S. Sanguinetti, Nat. Mater. **18**, 799 (2019).
[18]H. Z. Song, T. Usuki, S. Hirose, K. Takemoto, Y. Nakata, N. Yokoyama, and Y. Sakuma, Appl. Phys. Lett. **86**, 113118 (2005).
[19]P. Holewa, J. Jasiński, A. Shikin, E. Lebedkina, A. Maryński, M. Syperek, and E. Semenova, Materials **14**, 391 (2021).
[20]K. D. Jöns, P. Atkinson, M. Müller, M. Heldmaier, S. M. Ulrich, O. G. Schmidt, and P. Michler, Nano Lett. **13**, 126 (2013).
[21]Z. M. Wang, B. L. Liang, K. A. Sablon, and G. J. Salamo, Appl. Phys. Lett. **90**, 113120 (2007).
[22]R. Keil, M. Zopf, Y. Chen, B. Höfer, J. Zhang, F. Ding, and O. G. Schmidt, Nat. Commun. **8**, 15501 (2017).
[23]C. Heyn, Phys. Rev. B **83**, 165302 (2011).
[24]C. Heyn, A. Stemmann, R. Eiselt, and W. Hansen, J. Appl. Phys. **105**, 054316 (2009).
[25]C. Heyn, A. Küster, M. Zocher, and W. Hansen, Phys. Status Solidi RRL **13**, 1800245 (2019).
[26]C. Heyn, T. Bartsch, S. Sanguinetti, D. Jesson, and W. Hansen, Nanoscale Res. Lett. **10**, 67 (2015).
[27]C. Heyn, M. Zocher, S. Schnüll, and W. Hansen, Nanoscale Res. Lett. **11**, 428 (2016).
[28]C. Heyn, M. Zocher, L. Pudewill, H. Runge, A. Küster, and W. Hansen, J. Appl. Phys. **121**, 044306 (2017).
[29]M. Zocher, C. Heyn, and W. Hansen, J. Cryst. Growth **512**, 219 (2019).
[30]A. Stemmann, T. Köppen, M. Grave, S. Wildfang, S. Mendach, W. Hansen, and C. Heyn, J. Appl. Phys. **106**, 064315 (2009).
[31]Y. H. Huo, A. Rastelli, and O. G. Schmidt, Appl. Phys. Lett. **102**, 152105 (2013).
[32]E. Schöll, L. Hanschke, L. Schweickert, K. D. Zeuner, M. Reindl, S. F. Covre Da Silva, T. Lettner, R. Trotta, J. J. Finley, K. Müller, A. Rastelli, V. Zwiller, and K. D. Jöns, Nano Lett. **19**, 2404 (2019).
[33]F. Olbrich, J. Kettler, M. Bayerbach, M. Paul, J. Höschele, S. L. Portalupi, M. Jetter, and P. Michler, J. Appl. Phys. **121**, 184302 (2017).
[34]T. Müller, J. Skiba-Szymanska, A. B. Krysa, J. Huwer, M. Felle, M. Anderson, R. M. Stevenson, J. Heffernan, D. A. Ritchie, and A. J. Shields, Nat. Commun. **9**, 862 (2018).
[35]A. Musiał, P. Holewa, P. Wyborski, M. Syperek, A. Kors, J. P. Reithmaier, G. Sęk, and M. Benyoucef, Adv. Quantum Technol. **3**, 1900082 (2020).
[36]E. M. Sala, Y. I. Na, M. Godsland, A. Trapalis, and J. Heffernan, Phys. Status Solidi RRL **14**, 2000173 (2020).
[37]P. Holewa, S. Kadkhodazadeh, M. Gawełczyk, P. Baluta, A. Musiał, V. G. Dubrovskii, M. Syperek, and E. Semenova, "Droplet epitaxy symmetric InAs/InP quantum dots for quantum emission in the third telecom window: morphology, optical and electronic properties," Nanophotonics (2022).
[38]A. Chellu, J. Hilska, J.-P. Penttinen, and T. Hakkarainen, APL Mater. **9**, 051116 (2021).
[39]J. Hilska, A. Chellu, and T. Hakkarainen, Cryst. Growth Des. **21**, 1917 (2021).
[40]M. Zocher, C. Heyn, and W. Hansen, J. Appl. Phys. **125**, 025306 (2019).
[41]S. Lee, S. T. Choi, and Y. Y. Earmme, Int. J. Solids Struct. **45**, 746 (2008).
[42]M. K. Hudait, Y. Lin, M. N. Palmisiano, C. Tivarus, J. P. Pelz, and S. A. Ringel, J. Appl. Phys. **95**, 3952 (2004).
[43]R. Kumar and D. Biswas, Cryst. Res. Technol. **51**, 723 (2016).
[44]R. Kumar, A. Bag, P. Mukhopadhyay, S. Das, and D. Biswas, Appl. Surf. Sci. **357**, 922 (2015).
[45]G. Ju, H. Kim, J.-P. Shim, S. K. Kim, B.-h. Lee, S. O. Won, S. Kim, and H.-j. Kim, Thin Solid Films **649**, 38 (2018).
[46]S. Paul, J. B. Roy, and P. K. Basu, J. Appl. Phys. **69**, 827 (1991).
[47]K. Samonji, H. Yonezu, Y. Takagi, and N. Ohshima, J. Appl. Phys. **86**, 1331 (1999).
[48]Y. Yu, H. Zhong, J. Yang, L. Liu, J. Liu, and S. Yu, Nanotechnology **30**, 485001 (2019).
[49]R. Goodall, Data Brief **26**, 104515 (2019).

© Author(s) 2022